JGR Atmospheres

RESEARCH ARTICLE
10.1029/2022JD037282

# On the Intensity of First Return Strokes in Positive Cloud-To-Ground Lightning in Winter

**Ting Wu**[1], **Daohong Wang**[1], **and Nobuyuki Takagi**[1]

[1]Department of Electrical, Electronic and Computer Engineering, Gifu University, Gifu, Japan

**Key Points:**

- The intensity of first positive return strokes (RSs) is positively correlated with rise time and pulse width of E-change waveforms of the RSs
- The intensity of first positive RSs is related with the preliminary breakdown and preceding leader processes
- Strongest positive RSs usually occur in a short time (<10 ms) after lightning initiation, preceded by a fast (~$10^6$ m/s) positive leader

**Supporting Information:**

Supporting Information may be found in the online version of this article.

**Correspondence to:**

T. Wu,
tingwu@gifu-u.ac.jp

**Citation:**

Wu, T., Wang, D., & Takagi, N. (2022). On the intensity of first return strokes in positive cloud-to-ground lightning in winter. *Journal of Geophysical Research: Atmospheres*, *127*, e2022JD037282. https://doi.org/10.1029/2022JD037282

Received 10 JUN 2022
Accepted 2 NOV 2022

© 2022. American Geophysical Union. All Rights Reserved.

**Abstract** Intensities of about 700 first return strokes (RSs) in positive cloud-to-ground lightning flashes observed by a 14-site Fast Antenna Lightning Mapping Array in one winter season are analyzed. Peak currents estimated from range-normalized peak amplitudes of electric field change (E-change) waveforms of RSs are used to represent their intensities. It is found that peak currents of positive RSs are positively correlated with their waveform parameters including pulse width, rise time, fall time and half-peak width. Time differences between lightning initiation and first RSs are closely related with peak currents of positive RSs, with strong positive RSs usually associated with small time differences. Peak currents of positive RSs are also related with amplitudes of preceding leader pulses. Out of 674 positive RSs, 232 are preceded by positive leader pulses, and amplitudes of these pulses are positively correlated with peak currents of RSs. Strong positive RSs with peak currents larger than 150 kA are analyzed and compared with strong negative RSs. While strong negative RSs usually produce abnormal E-change waveforms that are generally different from typical RS waveforms, strong positive RSs do not have such special features. Strongest positive RSs usually occur within a very short time (usually smaller than 10 ms) after lightning initiation and are more likely to be associated with positive preliminary breakdown pulses. It is inferred that these strongest RSs are usually preceded by a fast downward positive leader with a speed on the order of $10^6$ m/s. Charge structures responsible for strong positive RSs are discussed.

**Plain Language Summary** It is well known that positive return strokes (RSs) are more likely to be very strong compared with negative RSs, but the reason is not clear. In this study, we analyzed the intensity of about 700 first RSs in positive cloud-to-ground lightning flashes and investigated its relationship with other parameters and discharge processes. With such a large sample, we demonstrated that strong positive RSs are usually associated with short time differences with lightning initiation and strong preceding leader pulses. Particularly, the strongest positive RSs usually occur within a few milliseconds after lightning initiation and are usually preceded by a fast downward positive leader with a speed on the order of $10^6$ m/s. It is speculated that a strong downward electric field near the ground is essential for the production of strong positive RSs. Possible charge structures responsible for strong positive strokes are proposed.

## 1. Introduction

The return stroke (RS) is usually the strongest discharge process in a cloud-to-ground (CG) lightning flash and is thought to be responsible for most lightning-related damages. Although RSs in negative CG flashes have been well studied, those in positive CG flashes are still poorly understood, largely due to the fact that positive CG flashes are much rarer than negative ones. Much knowledge about the intensity of positive RSs has been obtained with observations of nationwide lightning location systems such as the National Lightning Detection Network (NLDN) (e.g., Cummins & Murphy, 2009), and it has been well established that positive RSs are more likely to carry very large peak currents than negative ones (Lyons et al., 1998). This has been confirmed by space-based observations showing that the brightest lightning flashes are usually positive CG flashes (Peterson & Lay, 2020). However, these observations cannot provide detailed information on characteristics of individual lightning flashes, so it is not clear if positive CG flashes producing strong RSs have any common characteristics, which is a key question for understanding the mechanism responsible for large peak currents in positive RSs.

Some advancements have been made in understanding intensities of RSs in negative CG flashes, which are much more common. Shi et al. (2019), based on 3-D lightning mapping results of 279 negative CG flashes, reported that the intensity of first RSs in negative CG flashes is related with preceding discharge processes including the preliminary breakdown (PB) and stepped leaders. Their key finding is that strong negative RSs are usually

preceded by a fast stepped leader. The same conclusion can also be inferred from analyses of electric field change (E-change) waveforms of negative CG flashes (Nag & Cummins, 2017; Zhu et al., 2015, 2016). A similar result has also been reported for positive CG flashes by Wang et al. (2021) based on the analysis of 24 positive CG flashes observed by the Lightning Mapping Array (Rison et al., 1999) in winter.

Recently, Wu, Wang, Huang, and Takagi (2021) reported that negative RSs with peak currents larger than 150 kA in winter produce abnormal E-change waveforms that are generally different from those of typical RSs. Due to the abnormal waveforms, these strong discharges had not been recognized as RSs by the lightning research community. This finding raised a new question: do strong positive RSs produce abnormal E-change waveforms as well?

In this paper, we will analyze the intensity of about 700 first RSs in positive CG flashes observed in winter by the Fast Antenna Lightning Mapping Array (FALMA). Based on this large data set, we will investigate the relationship between the intensity of first positive RSs and characteristics of RS waveforms, PB and preceding leader pulses. Special attention will be paid to strong positive RSs with peak currents larger than 150 kA, and a comparison with strong negative RSs will be made.

## 2. Observation and Data

Data analyzed in this paper were recorded by a 14-site FALMA during the winter observation in the Hokuriku region of Japan from December 2018 to March 2019. The FALMA is a 3-D lightning mapping system using the fast antenna as the sensor, working in the frequency band of 500 Hz to 500 kHz (Wu et al., 2018a). During the winter observation, however, source height results are not reliable as discussed by Wu et al. (2020), so we will only use 2-D mapping results in this paper. With the 2-D mapping results, we can unambiguously determine PB and leader pulses that belong to the same flash as an RS. Observation sites of the FALMA during the winter observation are shown as black squares in Figure 1a.

All identified first RSs in positive CG flashes in a $200 \times 200$ km$^2$ region are shown in Figure 1a. RSs represented by red cross signs in Figure 1a are those saturating all FALMA sites so their peak currents could not be estimated and are not included in this study. The remaining 690 RSs are represented by colored plus signs with the color indicating the peak current and will be analyzed in this paper. Note that positive CG flashes analyzed in this study include bipolar CG flashes starting with a positive RS but do not include those starting with a negative RS. Also note that the number of RSs used in different analyses will be slightly different as the data requirements for different analyses are different. Details will be provided at the beginning of each analysis in Section 3.

Peak currents of RSs are estimated from range-normalized peak amplitudes of E-change waveforms of RSs. Simply speaking, range-normalized peak amplitudes of some RSs measured by the FALMA were compared with peak currents reported by the Japan Lightning Detection Network (JLDN) (e.g., Matsui et al., 2019) to calculate a conversion coefficient (we purchased the JLDN data in a 4-hr period with frequent lightning activities), then peak currents of all RSs recorded by the FALMA can be calculated from range-normalized peak amplitudes and the conversion coefficient. The detailed procedure for the current estimation was described by Wu, Wang, and Takagi (2021). Figure S1 in the Supporting Information shows peak currents of RSs versus distances (relative to the origin in Figure 1a). We can see that peak currents are generally not related with distances, indicating that there is no distance-related bias in the estimation of peak currents.

Positive RSs are all manually identified by their E-change waveforms. We did not set any quantitative criterion on waveform characteristics for the identification, because any criterion would inevitably result in certain biases in distributions of waveform characteristics and peak currents. Although manual identification will also introduce certain errors, we believe this is the most accurate, though laborious, way to identify RSs. Waveforms of all identified positive RSs are provided in the data repository so readers can see what events have been analyzed in this paper.

The physics sign convention is used in this paper, so a positive RS produces an initial positive electric field change.

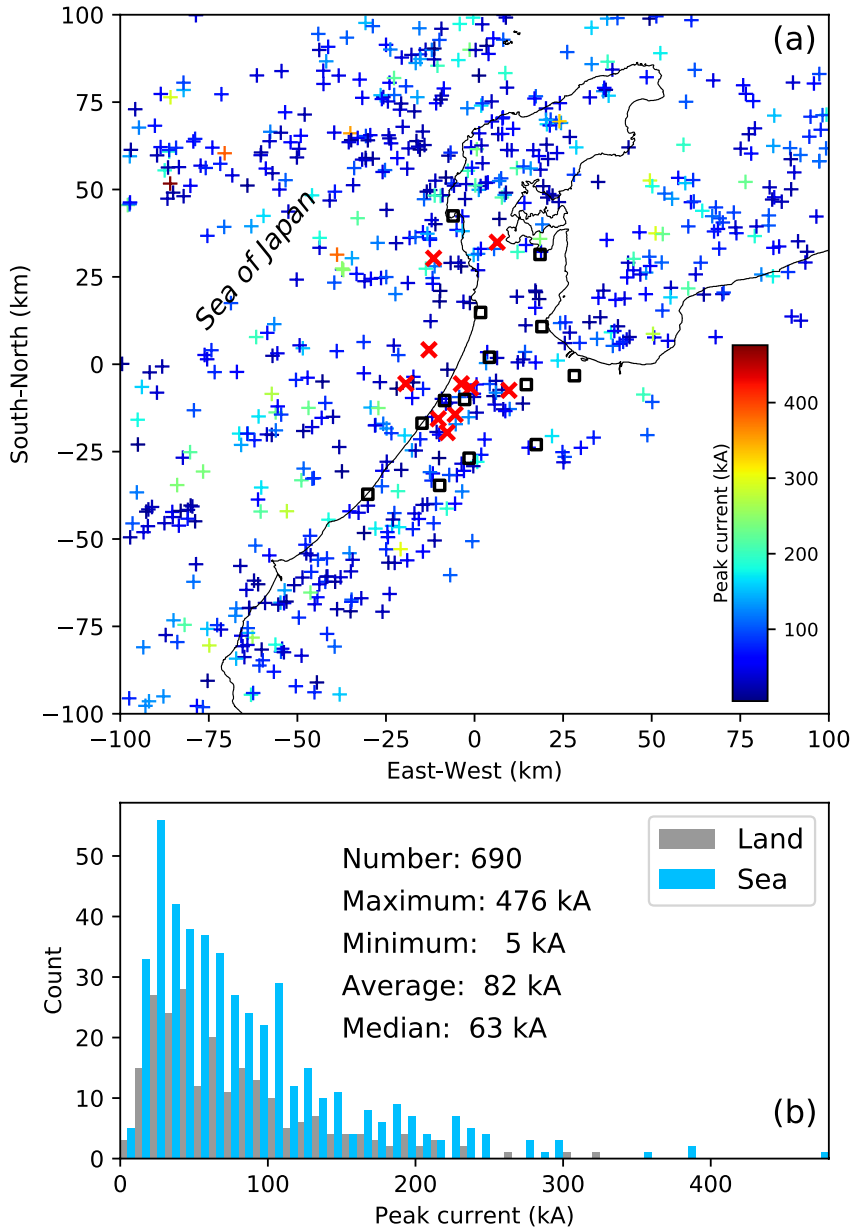


**Figure 1.** (a) Locations of all first RSs in positive CG flashes. The color indicates the estimated peak current of the RS. Red crosses represent RSs saturating all observation sites. Black squares represent observation sites of the FALMA. The origin (0, 0) corresponds to the latitude and longitude of (36.76°N, 136.76°E). (b) Distributions of peak currents. Gray bars represent first positive RSs on land and blue bars on the sea.

## 3. Results

### 3.1. Peak Current Statistics of Positive Return Strokes

The distribution of peak currents of all 690 first RSs in positive CG flashes is shown in Figure 1b along with some statistical results. The maximum current is 476 kA and the minimum is 5 kA. The average value is 82 kA and the median value is 63 kA. These values are generally higher than statistical results reported by nationwide lightning location systems such as the NLDN (Orville et al., 2011; Rudlosky & Fuelberg, 2010; Wacker & Orville, 1999). It is possible that some relatively weak positive RSs were not identified in this study, resulting in an overestimation of the statistical results, but it is also possible that positive RSs in winter thunderstorms in Japan are stronger than those in other regions and seasons. Moreover, the focus of this study is to investigate possible parameters

and discharge processes related with peak currents of positive RSs, so the possible overestimation will have very limited influence.

In Figure 1b, gray bars represent RSs on land and blue bars represent RSs on the sea. There are 227 RSs on land and 463 RSs on the sea. There are no clear differences between peak current distributions of RSs on land and on the sea. For the 227 RSs on land, the average value of the peak current is 77 kA and the median value is 63 kA. The average and median values for the 463 RSs on the sea are 85 and 64 kA. Although average values show certain difference, median values are very close for RSs on land and on the sea. It is well known that unlike negative RSs, peak currents of positive RSs on land and on the sea do not have clear systematic differences (Chronis et al., 2016; Orville et al., 2011).

### 3.2. Relationship Between Peak Current and Return Stroke Waveform

The relationship between peak currents of first positive RSs and parameters of their E-change waveforms is investigated. In order to reduce the influence of distortions due to the static field component and local noises, only first RSs farther than 50 km from at least two sites are included in this analysis. There are a total of 623 events satisfying this condition. For each waveform parameter, waveforms recorded by all sites farther than 50 km away from the event are used to calculate the parameter, and their median value is used as the result of the parameter. Definitions of waveform parameters including pulse width, rise time and fall time are the same as those in Wu, Wang, Huang, and Takagi (2021).

Relationships between peak currents and parameters of RS waveforms are shown in Figure 2. RSs on land and on the sea are represented by gray and blue points, respectively. The value of $r$ represents the Pearson correlation coefficient for each pair of parameters. Positive correlations can be seen between peak current and pulse width, rise time, fall time, and half-peak width. The correlation is strongest for the rise time. The positive correlation between the peak current and the rise time was also reported for negative first RSs (Nag & Cummins, 2018). These moderate or strong positive correlations in Figure 2 (except of the correlation for the ratio of fall time to rise time in Figure 2e) may be simply because an RS with a larger peak current generally needs a longer time for the current to reach the peak. However, these correlations indicate a fundamental difference from waveform characteristics of strong negative RSs in winter. Wu, Wang, Huang, and Takagi (2021) reported that strong negative RSs with peak currents larger than 150 kA produce E-change waveforms that are generally different from normal RSs. Particularly, their pulse width and fall time are generally smaller than those of normal RS waveforms. From Figure 2, we can see that E-change waveforms of strong positive RSs do not have this special feature.

Figure 2 also shows distributions and statistical results of waveform parameters. Statistical results of waveform pamameters of positive RSs have been reported by many studies, and our results are generally consistent with previous studies (e.g., Nag & Rakov, 2014; Qie et al., 2013; Schumann et al., 2013). From Figure 2 we can also see that distributions of waveform parameters of RSs on land and on the sea do not show clear differences. Although it is expected that upward connecting leaders on land and on the sea may have certain differences due to different surface conditions, this result indicates that different surface conditions of the land and the sea have very limited influences on E-change waveforms of positive RSs.

### 3.3. Relationship Between Peak Current and Preliminary Breakdown

Relationships between peak currents of positive RSs and various properties of PB pulses are investigated, and the results are shown in Figure 3. It should be noted that some positive CG flashes did not start with PB pulses or PB pulses were too weak to determine their properties, and these cases are excluded, and finally 673 cases are included in this analysis. E-change waveforms of one typical flash that did not start with PB pulses are shown in Figure 4b. We can see that this flash started with some weak pulses with very large pulse widths, which are distinctly different from typical PB pulses.

It is well known that positive CG flashes can start with positive PB pulses (the same polarity as positive RSs) or negative PB pulses. In this study, 317 positive flashes started with positive PB pulses and 356 started with negative PB pulses. This is consistent with the observation in winter by Wu et al. (2013) who observed 11 positive flashes starting with positive PB pulses and 15 with negative PB pulses, but it is different from the observation in winter by Ushio et al. (1998) that 17 out of 19 positive CG flashes started with positive PB pulses. Additionally,

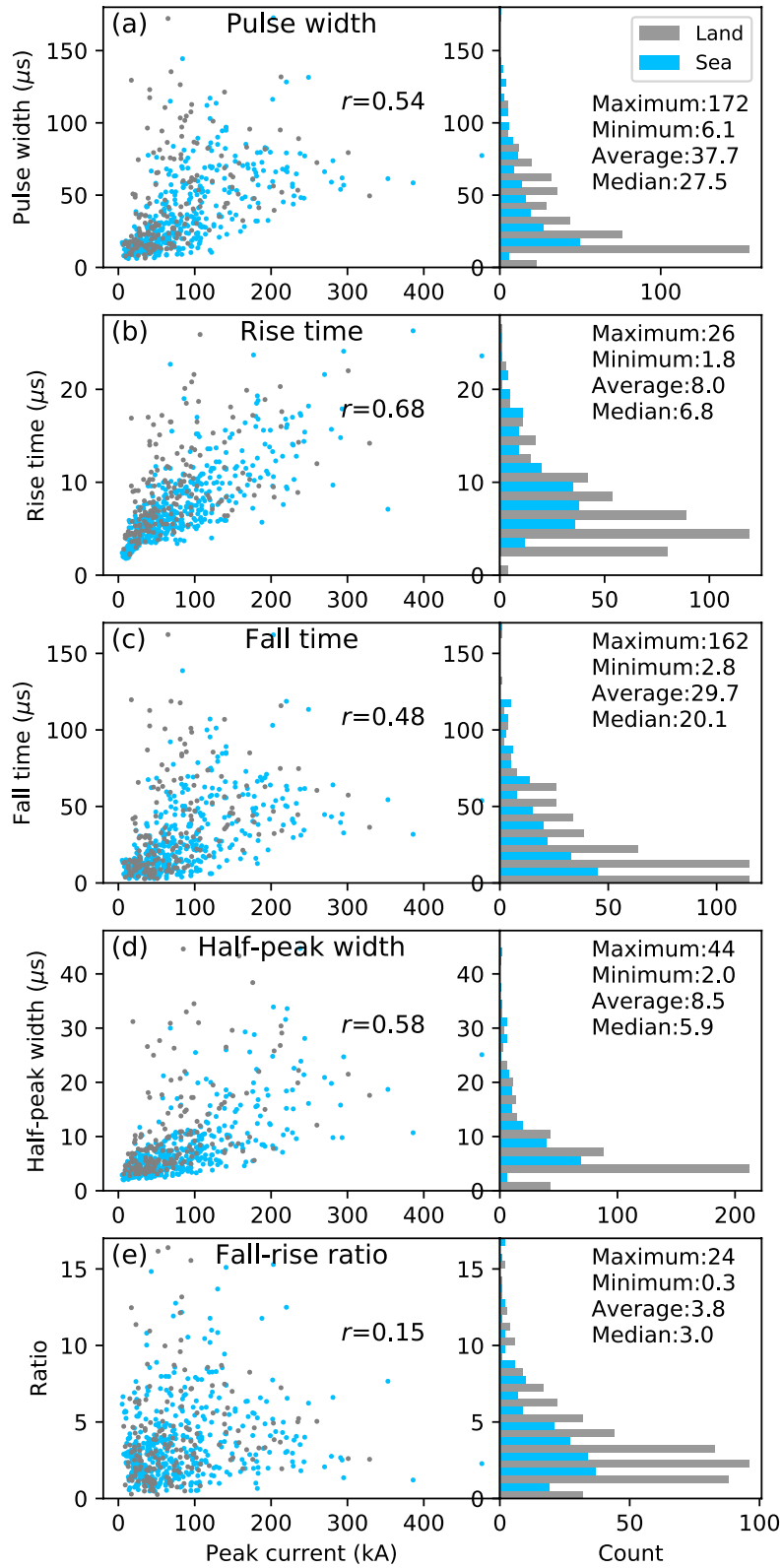


**Figure 2.** Relationship between peak currents of first positive RSs and (a) pulse width, (b) rise time, (c) fall time, (d) half-peak width, and (e) ratio of fall time to rise time of RS waveforms. Gray points and bars represent positive RSs on land and blue ones represent those on the sea. The event with the maximum value in (e) is not shown. The value of *r* represents the Pearson correlation coefficient.

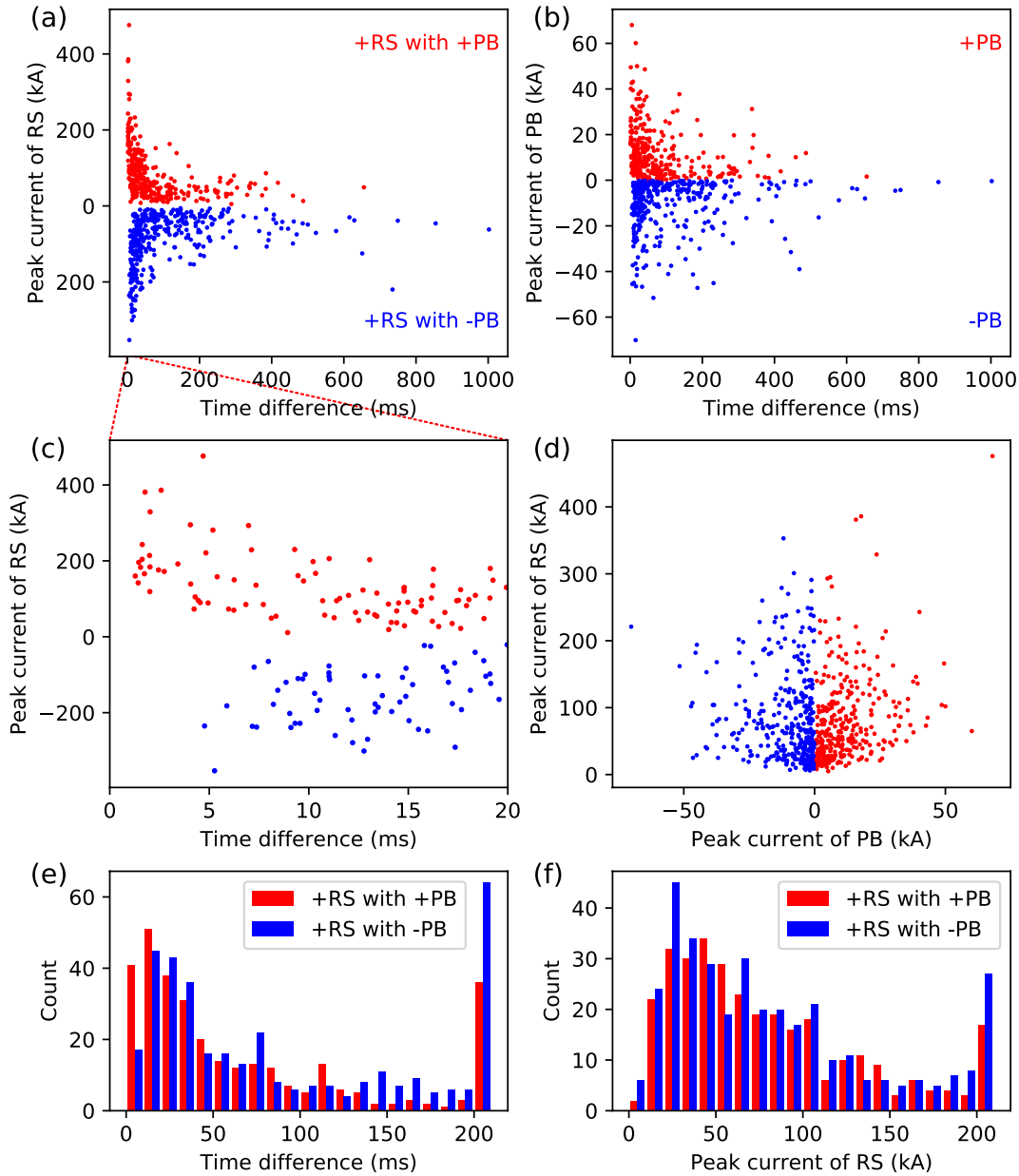


**Figure 3.** (a) Relationship between the time difference (from lightning initiation to the first positive RS) and the peak current of positive RSs. (b) Relationship between the time difference and the peak current of the PB (estimated peak current of the largest pulse in a PB pulse train). (c) The same as (a) but only shows the range of time differences from 0 to 20 ms. (d) Relationship between the peak current of PB and RS. (e) Distribution of the time difference. (f) Distribution of the peak current of RS. Red dots and bars represent positive PB pulses or RSs preceded by positive PB pulses, and blue ones represent negative PB pulses or RSs preceded by negative PB pulses.

there is evidence that positive CG flashes in summer thunderstorms, especially in low- and mid-latitude regions, mostly start with positive PB pulses (Nag & Rakov, 2012; Wu et al., 2018b; Zhang et al., 2013).

Figure 3a shows the relationship between the time difference (from the initiation of the positive CG flash to the first RS) and the peak current. The initiation of a positive CG flash is determined as the first pulse in a PB pulse train, and 2-D mapping results are used to determine the PB pulse train that belongs to the same flash as the first RS. Note that the first pulse of a flash is usually very small, likely corresponding to the so-called "initial E-change" reported by Marshall et al. (2014). A pronounced feature in Figure 3a is that RSs with large peak currents are usually associated with small time differences, which is true for flashes with both positive

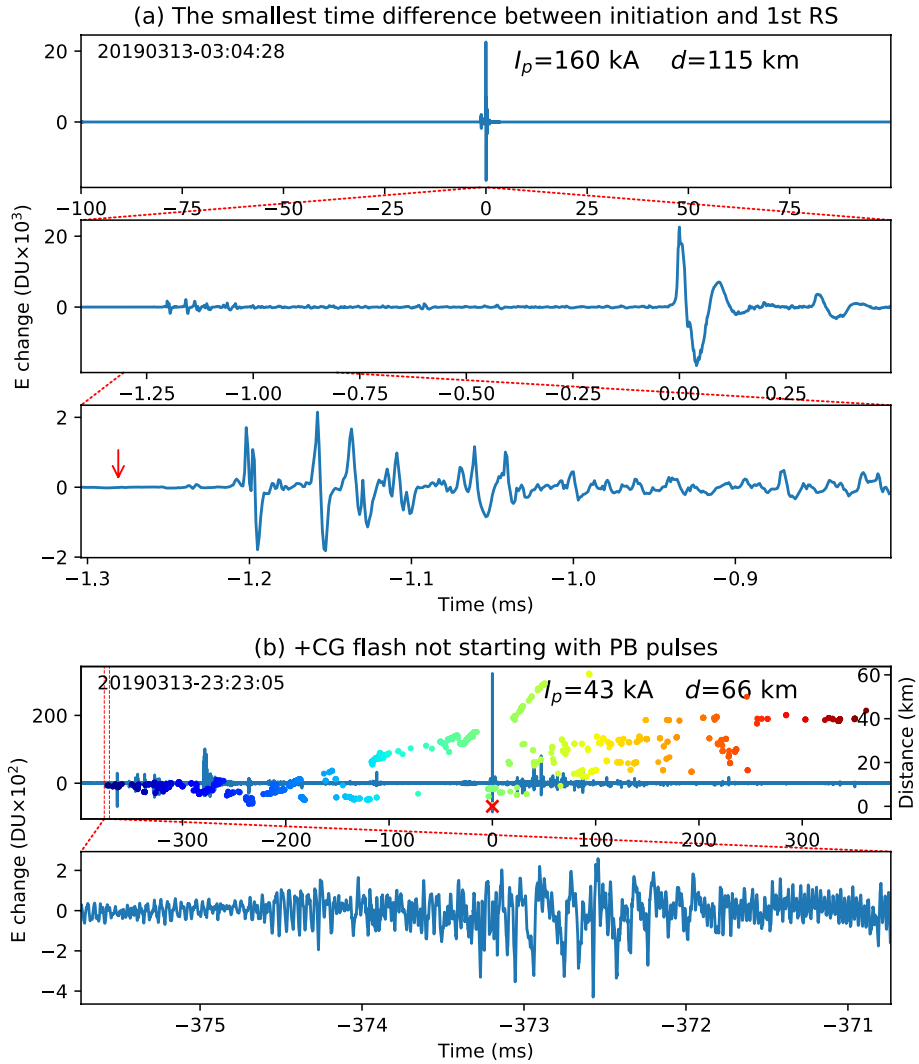


**Figure 4.** (a) E-change waveforms of the positive CG flash with the smallest time difference between the initiation and the first RS. $I_p$ is the peak current of the RS, and $d$ is the distance between the RS and the site recording the waveforms. The red arrow indicates the first pulse of this flash. (b) E-change waveforms of a positive CG flash starting without PB pulses. Colored points represent distances of located sources relative to the RS. The red cross sign indicates the RS. The time scale of the figure indicates that the initial pulses have very large pulse widths, different from PB pulses.

and negative PB pulses. In other words, if the peak current of the first RS in a positive CG flash is very large, it usually occurs soon after the initiation of the flash, no matter if the PB pulses are positive or negative. However, the opposite is not true; as we can see in Figure 3a, there are plenty of cases with both small peak currents and small time differences.

Although the correlation between the peak current and the time difference does not seem to be related with the polarity of PB pulses, positive PB pulses are more likely to be associated with extremely small time differences. Figure 3c shows the same result as Figure 3a but zooms in on the range of time differences from 0 to 20 ms. We can see that almost all cases with a time difference smaller than 5 ms are associated with positive PB pulses (25 cases with positive PB pulses compared with 1 case with negative PB pulses). The minimum time difference for cases with positive PB pulses is 1.28 ms while that for cases with negative PB pulses is 4.76 ms. The same result can also be seen in Figure 3e, which shows distributions of time differences for positive flashes with positive and negative PB pulses. We can see that although overall distributions are similar, positive PB pulses are more likely to be associated with very small time differences while negative PB pulses are more likely to be associated with very large time differences.

E-change waveforms of the positive stroke with the minimum time difference of 1.28 ms are shown in Figure 4a. The RS has a relatively large peak current of 160 kA. It is interesting to note that the duration of the whole flash is also extremely short; there are no signatures of discharges after the RS. Previous studies reported that the time difference between the initiation or the PB and the first RS in positive CG flashes is normally tens of milliseconds or larger than 100 ms in summer (e.g., Qie et al., 2013; Schumann et al., 2013; Zhang et al., 2013) and can be as short as several milliseconds in winter (Wu et al., 2013, 2020). We believe a positive RS with such a short time difference of 1.28 ms from lightning initiation is reported for the first time.

The relationship between the time difference and the peak current of the PB is also investigated and the result in shown in Figure 3b. The peak current of the PB is calculated from the E-change magnitude and the 2-D location of the largest PB pulse in a PB pulse train in the same manner as estimating RS peak currents. Therefore, the value is unlikely accurate as the true peak current flowing during the PB process, but it is likely well correlated with the peak current of the PB process. Figure 3b shows a similar, but weaker, relationship as that between the time difference and the peak current of RSs in Figure 3a. It indicates that strong PB pulses are usually followed by a positive RS in a short time. But again, the opposite is not true—weak PB pulses can be followed by a positive RS in either a very short or a very long time. Further, there is no clear correlation between the peak current of the PB and that of RSs as shown in Figure 3d. The only feature that can be determined from Figure 3d is that strong PB pulses are unlikely to be followed by very weak positive RSs. Finally, Figure 3f shows distributions of peak currents of positive RSs associated with positive and negative PB pulses. It shows that the polarity of PB pulses has little influence on the peak current of positive RSs overall. However, as will be discussed in Section 4, the strongest positive RSs are more likely to be associated with positive PB pulses.

### 3.4. Relationship Between Peak Current and Preceding Leader Pulses

The relationship between the peak current of positive RSs and the amplitude of pulses right before the RS is investigated. In this analysis, we include positive RSs observed by at least one site more than 50 km away, and there are a total of 674 positive RSs. Many positive RSs are preceded by positive pulses (the same polarity as the positive RS), but there are also many cases in which there are no identifiable pulses. For simplicity, we confine this analysis to pulses within 500 μs before the peak of the RS. Further, in order to avoid the influence of the onset of the RS pulse, we exclude pulses within 50 μs before the peak of the RS. Therefore, pulses in the period of −500∼−50 μs before the peak of the RS are manually inspected for the selected 674 cases. These cases are classified into three types: type 1—predominantly positive pulses, type 2—predominantly negative pulses, and type 3—no clear pulses or pulses with mixed polarities. We are aware that the classification is sometimes subjective, so figures showing the preceding pulses with the designated type for all events are provided in the data repository.

There are 232 positive RSs preceded by predominantly positive pulses. One typical example is shown in Figure 5a. By contrast, there are only 15 cases preceded by predominantly negative pulses. One case with clear negative pulses is shown in Figure 5b. In the remaining 427 cases, there are no clear preceding pulses or there are pulses of both polarities. Note that the waveform in Figure 5b may appear somewhat atypical as an RS pulse; it is determined as an RS pulse because of the fast rise to the peak and the fine structure after the peak, which are characteristic of RS pulses.

The peak current of preceding pulses is calculated and its correlation with the peak current of positive RSs is shown in Figure 6. Positive RSs on land are shown in Figure 6a and those on the sea in Figure 6b. For pulses of type 1, the amplitude of the largest positive pulse is used for the estimation of the peak current, and for pulses of type 2, the amplitude of the largest negative pulse is used. For pulses of type 3, the amplitude of the largest pulse, regardless of its polarity, is used. The peak current is estimated in the same manner as the estimation of the RS peak current.

From Figure 6, first we can see that most of type-3 pulses are associated with relatively weak RSs, mostly with peak currents smaller than 100 kA. For type-1 pulses, their peak currents have a clear positive correlation with peak currents of associated RSs. Particularly, strong positive pulses—for example, those with peak currents larger than 10 kA—are mostly associated with strong RSs with peak currents larger than 100 kA. Similarly, very strong RSs—for example, those with peak currents larger than 200 kA—are rarely associated with weak pulses.

Pulses right before positive RSs are thought to be produced by downward positive leaders or upward negative connecting leaders. Both situations would produce positive pulses, corresponding to type-1 pulses in Figure 6.

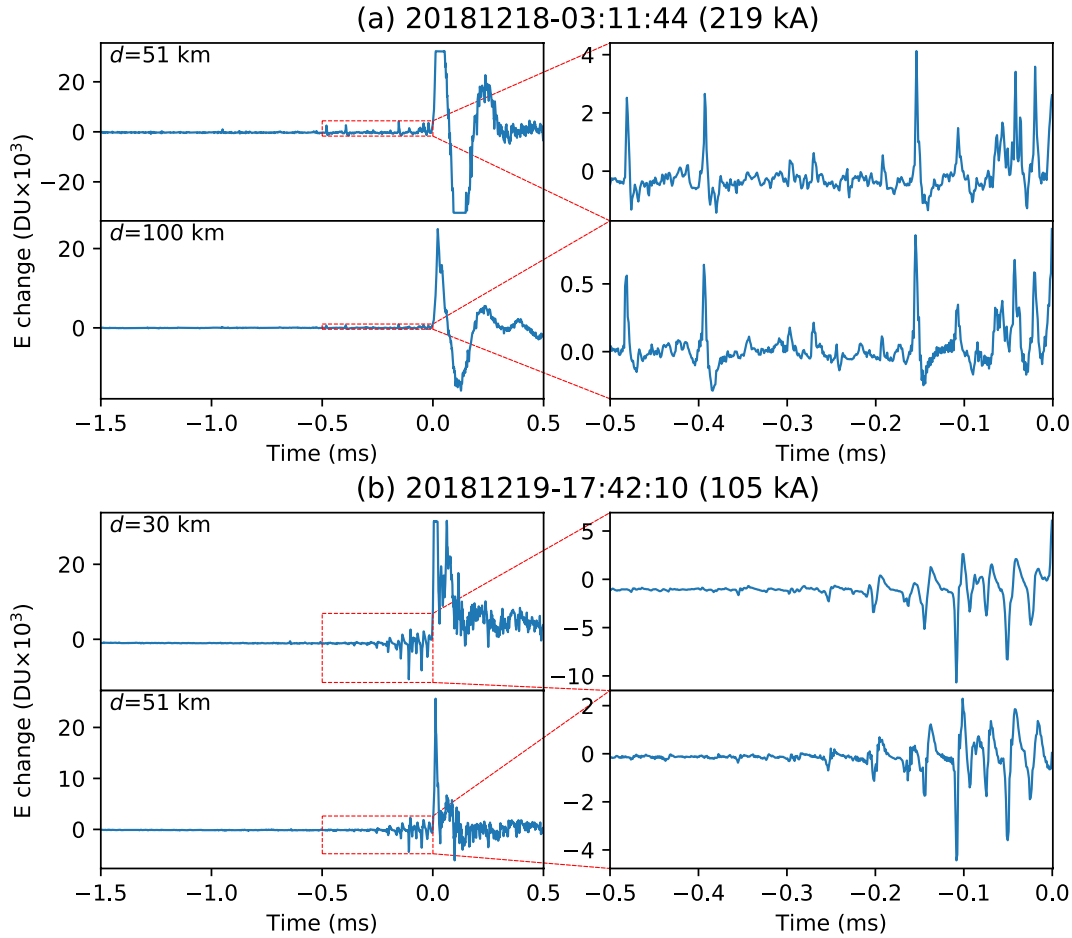


**Figure 5.** E-change waveforms of (a) a positive RS preceded by positive pulses and (b) a positive RS preceded by negative pulses. In each case, waveforms recorded by two sites with different distances are shown. The left part shows overall waveforms and the right part shows waveforms of preceding pulses.

And in both situations, the leader is quite close to the ground, so the pulse amplitude should be closely related with the strength of the electric field near the ground. Therefore, the correlation in Figure 6 indicates that the peak current of positive RSs is positively correlated with the electric field strength near the ground. This result agrees with the finding by Shi et al. (2019) that the peak current of negative RSs is positively correlated with the velocity of stepped leaders.

By comparing Figures 6a and 6b, we can see that correlations for positive strokes on land and on the sea have some differences, especially for type-1 pulses. It is clear that the positive correlation for type-1 pulses are much stronger when strokes are on the sea. This may be due to the fact that the sea surface is usually flat while the land surface is much more complicated, with various objects of different heights and shapes. The difference in Figures 6a and 6b may indicate that type-1 preceding pulses are mostly produced by upward negative connecting leaders rather than downward positive leaders, because upward connecting leaders are initiated from the ground and their characteristics are more likely to be influenced by grounded objects.

It is not clear why in some cases negative pulses occurred before positive RSs. As they only account for a very small percentage of recorded positive RSs, they may be produced in some special conditions. For example, the upward negative connecting leader may be highly tortuous and have a short period of downward propagation before connecting with the positive leader, or they may be produced by in-cloud negative leaders. It is also not clear why most negative pulses, including type-2 pulses and negative type-3 pulses, are associated with positive strokes on the sea as can be seen in Figure 6b.

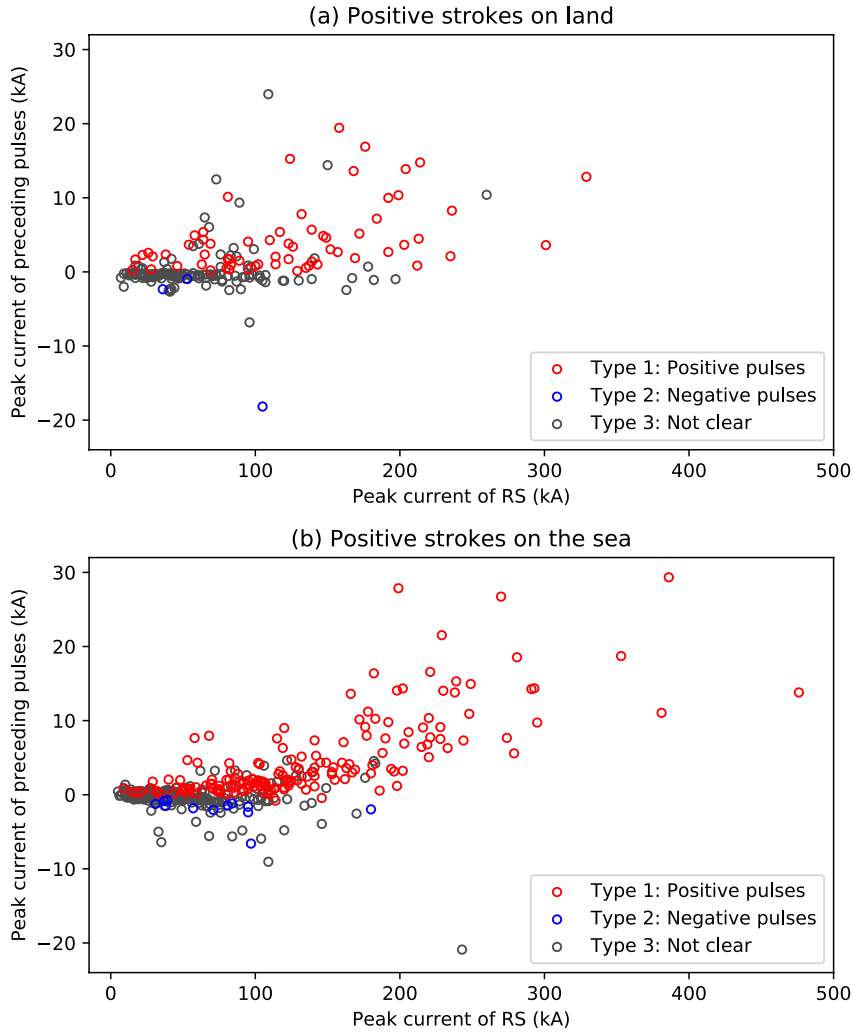


**Figure 6.** Relationship between peak currents of positive RSs and peak currents of preceding leader pulses within 0.5 ms before the RS for RSs (a) on land and (b) on the sea. Preceding pulses are classified into positive pulses (red circles), negative pulses (blue circles) and no identifiable pulses or pulses with mixed polarities (black circles).

### 3.5. Strong Positive Return Strokes and Comparison With Negative Ones

Wu, Wang, Huang, and Takagi (2021) analyzed strong negative RSs with peak currents larger than 150 kA in winter and found that their E-change waveforms are largely different from those of normal RSs. In this analysis, we will look at strong positive RSs with peak currents larger than 150 kA and compare them with negative ones.

Strong negative RSs analyzed by Wu, Wang, Huang, and Takagi (2021) are reanalyzed here. Note that Wu, Wang, Huang, and Takagi (2021) analyzed negative RSs in a region of $300 \times 300$ km$^2$, but positive RSs analyzed in this study are in a region of $200 \times 200$ km$^2$. Therefore, strong negative RSs reanalyzed in this study are also confined in the same $200 \times 200$ km$^2$ region as positive ones. There are 59 strong negative RSs in this region as shown in Figure 7a. Six of them saturated all observation sites as represented by red crosses, and the maximum peak current is 310 kA. By contrast, there are 104 strong positive RSs as shown in Figure 7b. Ten of them saturated all observation sites, and the maximum peak current is 476 kA. This result indicates that in winter thunderstorms in the Hokuriku region, strong positive RSs are much more frequent than negative ones, and they are more likely to carry extremely large peak currents.

Another difference that can be seen from Figure 7 is that compared with strong negative RSs, positive RSs are more likely to occur on the sea. In order to quantitatively analyze this feature, Figure 7c shows distributions of elevations (meters above sea level) at locations of different types of lightning discharges, including strong

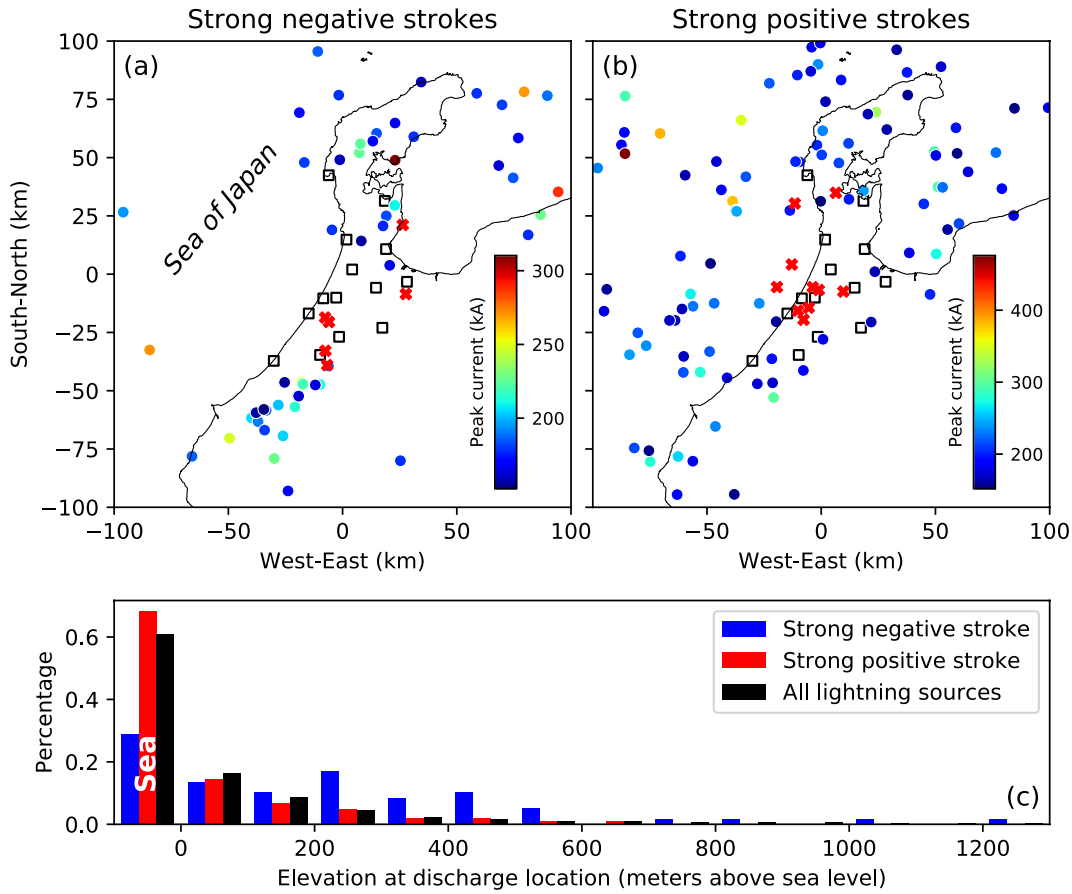


**Figure 7.** Locations of (a) strong negative RSs and (b) strong positive RSs with peak currents larger than 150 kA. Red crosses represent RSs saturating all observation sites. (c) Distributions of elevations at locations of strong negative RSs (blue bars), strong positive RSs (red bars) and all located discharge sources (black bars). Bars left of zero represent events on the sea.

negative RSs (those in Figure 7a), strong positive RSs (those in Figure 7b) and located sources of all lightning discharges in the same region. As winter thunderstorms usually develop from the Sea of Japan, move toward the land and dissipate soon after moving ashore and colliding with mountains, most lightning discharges in winter naturally occur on the sea as demonstrated by black bars in Figure 7c. Strong positive RSs (red bars) show a similar distribution, with the majority on the sea. This result likely indicates that strong positive RSs can be produced at any stage of thunderstorms in winter and their occurrences are not related with the topography. On the contrary, strong negative RSs have a much lower percentage on the sea, and percentages of RSs occurring at locations with elevations up to 500 m are consistently high, indicating that strong negative RSs tend to occur at areas with moderate elevations of a few hundred meters. In other words, moderate elevations of a few hundred meters are likely conducive to the production of strong negative RSs.

One interesting feature of strong negative RSs analyzed by Wu, Wang, Huang, and Takagi (2021) is that their E-change waveforms are largely different from those of normal negative RSs, leading to the consequence that some strong negative RSs were not recognized by nationwide lightning location systems. Here we will briefly look at E-change waveforms of strong positive RSs. Figure 8 shows E-change waveforms of the strongest 10 positive RSs analyzed in this paper. Generally speaking, waveforms of these RSs do not have any obvious difference with those of normal positive RSs. One clear tendency of these cases is that the time difference between the peak of the RS and the initiation of the flash ($\Delta t$ in Figure 8) is relatively small; in eight of these cases, $\Delta t$ is smaller than 10 ms. However, these time differences are still about one order of magnitude larger than those in strong negative strokes and can be hardly called abnormal. Another possible special common feature is that in many of these cases, some fine structures can be seen on the rising portion of RS pulses, which may have contributed to

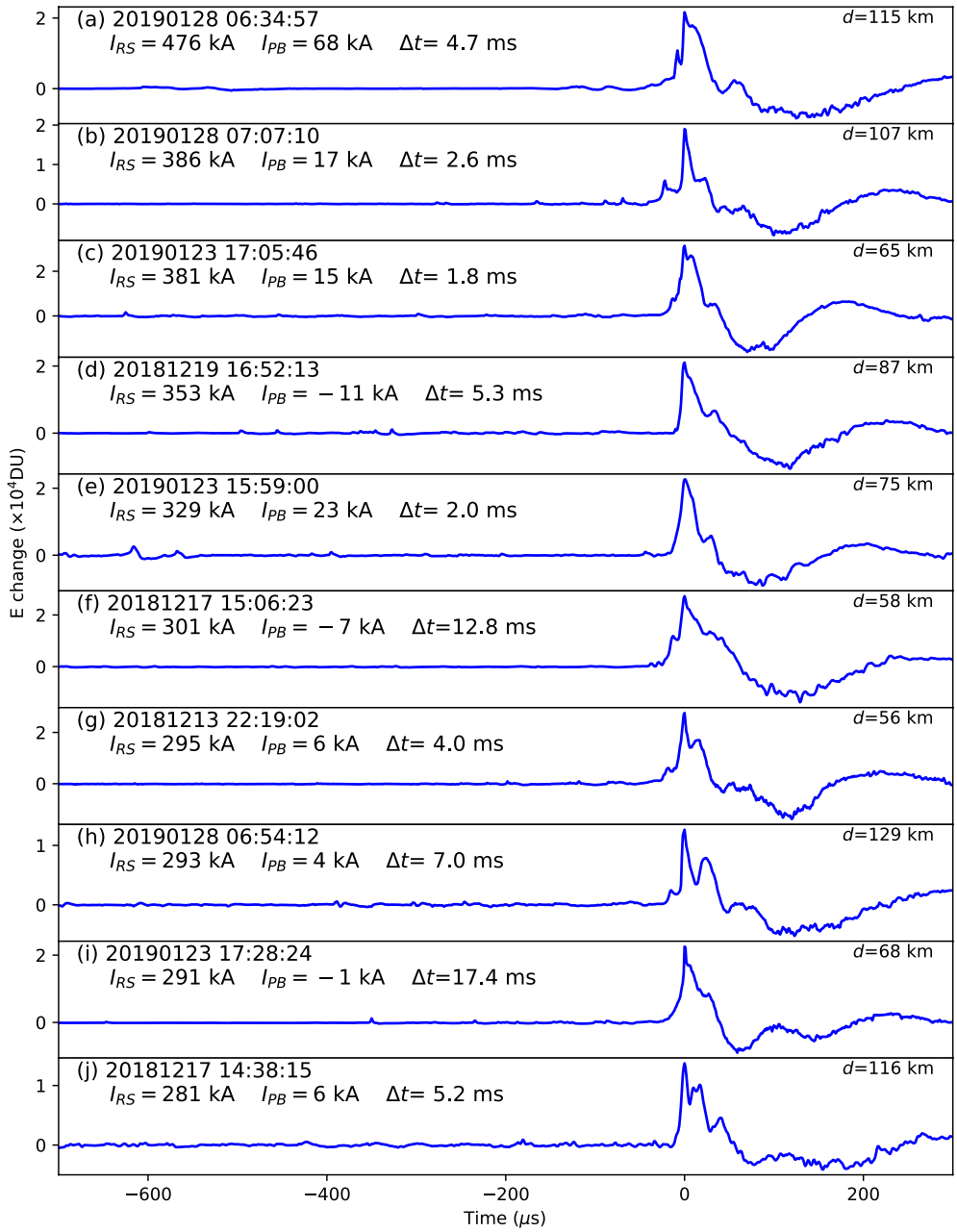


**Figure 8.** E-change waveforms of the 10 strongest positive strokes. $I_{RS}$ is the peak current of the positive RS. $I_{PB}$ is the peak current of the PB (not shown). Δ$t$ is the time difference between the initiation of the flash and the peak of the RS. $d$ is the distance of the RS to the site recording the plotted waveform.

large rise times for strong positive RSs as demonstrated in Figure 2b. Apart from these features, these waveforms are fairly typical positive RS waveforms and should be readily recognized by lightning location systems. We can also see from the relationships between RS waveform parameters and peak currents shown in Figure 2 that waveform characteristics of strong positive RSs do not have systematic differences with those of positive RSs with normal peak currents.

## 4. Conditions Favorable to the Production of Strong Positive Strokes

Based on the results described above, we can get some idea about the general characteristics of strong positive strokes and conditions favorable to their production. The most prominent feature of strong positive strokes is that the time difference between the initiation of the lightning flash and the RS is very short as demonstrated in Figure 3a. In other words, strong positive RSs usually occur very shortly after the initiation of the flash. This feature is also true for strong negative strokes in winter (Wu, Wang, Huang, & Takagi, 2021) as well as in summer (Nag & Cummins, 2017; Shi et al., 2019; Zhu et al., 2015, 2016). It is likely that the positive leader connecting to the ground is initiated at or shortly after the initiation of the flash and progresses with a high speed down to the ground.

In order to further analyze leader activities preceding strong positive RSs, Figure 9 shows scatterplots of the distance versus time for sources before and after some of the strongest positive RSs. Six of the ten cases in Figure 8 with relatively good location results are selected. The distance and the time are calculated relative to the RS represented by a black cross sign at (0, 0), and the first source of the flash is represented by a red diamond sign. Blue and red dashed lines represent velocities of $10^5$ and $10^6$ m/s, respectively. Located sources are generally produced by negative leaders. We can see that a common feature in these cases is a negative leader propagating away from the location of the RS with a high speed on the order of $10^6$ m/s. RSs usually occur only a few milliseconds after the lightning initiation and usually have a small horizontal distance of a few kilometers. We can roughly estimate the speed of the positive leader connecting to the ground with some assumptions. First, we assume the positive leader is initiated at the very beginning of the flash. Second, we assume the positive leader propagates in a straight line to the RS location. Third, we neglect the initiation height. All these assumptions will result in underestimations of the estimated speed. With these assumptions, the speed of the positive leader would be equal to the slope of the line connecting the initiation source (red diamond) and the RS (black cross) in Figure 9, and we can see from Figure 9 that in most of these cases the speed is very close to $1 \times 10^6$ m/s. Considering the assumptions, the actual speed may be well larger than $1 \times 10^6$ m/s. Downward positive leaders with speeds on the order of $10^6$ m/s have been reported before (Chen et al., 2015; Li et al., 2020; Pu et al., 2021; Wang & Takagi, 2011), but it seems that those with speeds well smaller than $10^6$ m/s are much more common (Saba et al., 2010). Furthermore, these previous observations correspond to the final stage of downward positive leaders right before connecting to the ground, so their overall speeds including in-cloud propagations are likely much smaller. Therefore, our estimation indicates that these strongest positive RSs are preceded by very fast positive leaders, and we can infer that before very strong positive RSs, there is usually a positive leader initiated at or shortly after the flash initiation and propagating downward to the ground with a large speed on the order of $10^6$ m/s. There is likely a fast negative leader as well with a speed on the order of $10^6$ m/s which continued propagating for a large distance after the positive RS. It should be noted that as we cannot estimate leader speeds for all positive strokes, especially those with large time differences from lightning initiations, we cannot exclude the possibility that downward positive leaders with speeds on the order of $10^6$ m/s are actually very common in winter.

Of the 10 strongest positive strokes shown in Figure 8, seven are preceded by positive PB pulses. Although peak currents of positive RSs associated with positive and negative PB pulses have very similar distributions as shown in Figure 3f, it seems positive RSs associated with positive PB pulses are more like to be extremely strong as can also be seen in Figure 3c. It is well understood that positive PB pulses are produced by upward negative leaders and negative PB pulses by downward negative leaders (Wu et al., 2018b). In the case of positive PB pulses, the initial negative leader propagates upward and the initial positive leader, though undetected, likely propagates downward. On the other hand, in the case of negative PB pulses, the initial negative leader always starts with a downward propagation, usually followed by an upward propagation (Wu et al., 2018b). The initial positive leader likely starts with an upward propagation, followed by a downward propagation toward the ground. Therefore, positive RSs associated with positive PB pulses are more likely to occur in a very short time after the lightning initiation as was demonstrated in Figure 3c, and they are apparently more likely to be associated with very strong downward electric fields.

Another feature of strong positive strokes is that they are usually associated with strong positive leader pulses right before RSs as demonstrated in Figure 6. As analyzed in Section 3.4, positive pulses preceding positive RSs are likely produced by upward negative connecting leaders, and strong positive pulses likely indicate a strong downward electric field near the ground.

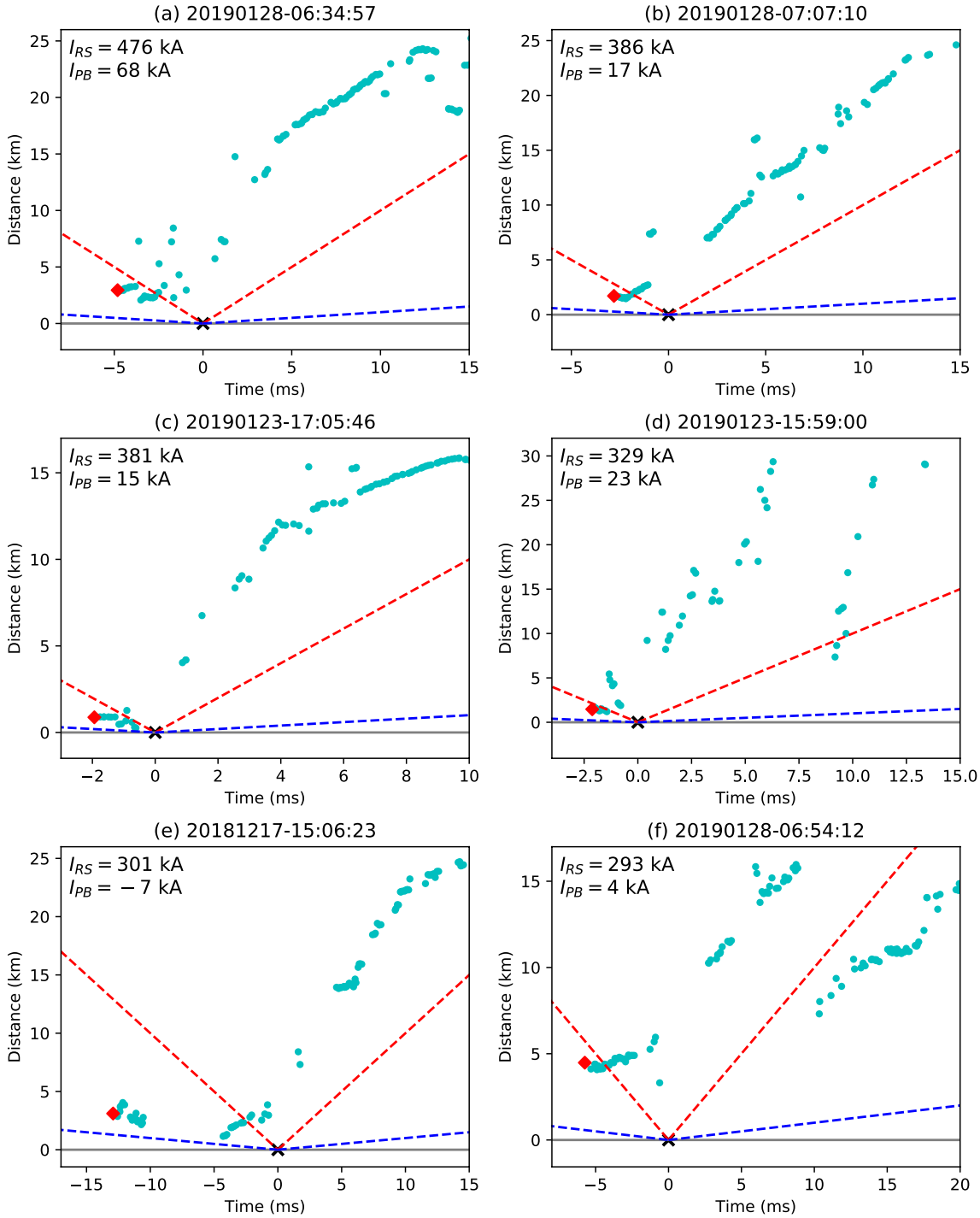


**Figure 9.** Scatterplots of the distance versus time for sources before and after some strong positive RSs. The distance and the time are calculated relative to the RS shown at (0, 0). The red diamond sign is the first source of +CG flashes. Blue and red dashed lines represent velocities of $10^5$ and $10^6$ m/s, respectively. $I_{RS}$ is the peak current of positive RSs. $I_{PB}$ is the peak current of the PB pulses before positive RSs.

Based on the above analyses, we can see that a strong downward electric field below the thundercloud, particularly near the ground, is the most essential factor in the production of strong positive strokes. Such a strong downward electric field can be produced by a positive charge region in the lower region of a thundercloud. The positive charge region likely has a fairly large horizontal extent as indicated by the large propagation distances of negative leaders shown in Figure 9. In the cases of strong positive strokes starting with positive PB pulses, the

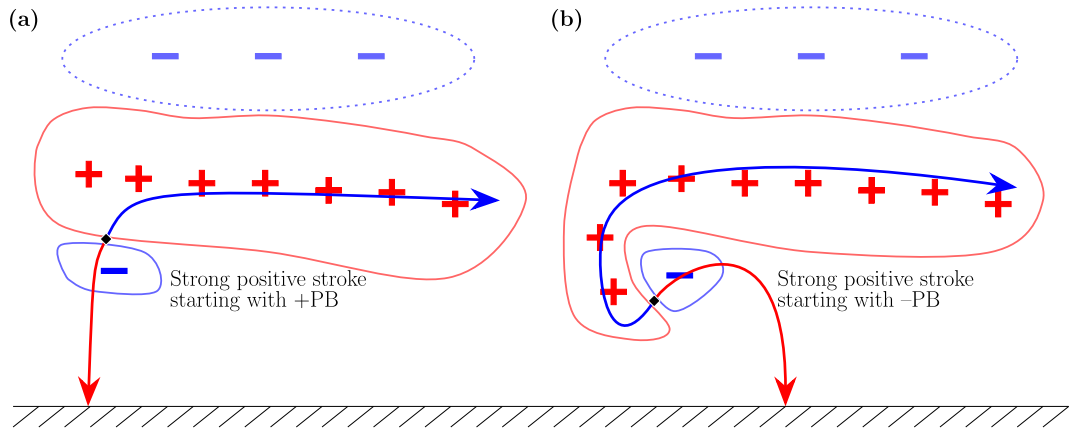


**Figure 10.** Illustrations of possible charge structures for strong positive strokes starting with (a) positive PB and (b) negative PB. Blue and red arrows represent negative and positive leaders, respectively.

initial positive leader propagates downward, so it is likely that there is a small negative "pocket" charge region below the positive charge region. The negative charge region is likely very small as it would reduce the downward electric field. A possible charge structure is shown in Figure 10a. Note that there may also be a main negative charge region above the positive charge region, forming an inverted tripolar charge structure. As the data in this study cannot show much information about the main negative charge region, it is shown as a dashed-line ellipse in Figure 10. Wang et al. (2021) also reported that most positive CG flashes in winter are associated with inverted charge structures, different from the traditional explanation that positive CG flashes in winter are associated with a normal charge structure in which the upper positive charge region is horizontally displaced from the negative charge region due to the strong wind shear (Brook et al., 1982).

For strong positive strokes starting with negative PB pulses, however, the initial positive leader needs to first propagate upward and soon turn downward. Such complicated behavior indicates a complicated charge structure. However, it is well known that charge structures in winter thunderstorms are usually very complicated (Wang et al., 2018; Zheng et al., 2019), which is likely the reason that positive CG flashes starting with positive and negative PB pulses are equally common in winter. A possible charge structure is proposed in Figure 10b, which shows a small negative charge region surrounded by a large positive charge region. The initiation location is at the lower side of the negative charge region, below which there are also some positive charges, so the initial negative leader starts with a downward propagation, producing negative PB pulses. The initial positive leader first propagates upward in the small negative charge region. Soon it gets out of the negative charge region, and under the strong downward electric field caused by the large positive charge region above, it turns downward to the ground with a fast speed.

It is easy to explain why positive RSs occurring a long time after the lightning initiation can rarely be very strong as can be seen in Figure 3a. Positive leaders initiating these RSs are more likely to develop from a negative leader channel after the negative leader propagated for a long time (Velde et al., 2014) and are thus far away from the location of the lightning initiation, where the electric field is supposed to be the strongest, and a relatively weak electric field results in a relatively weak RS. An alternative explanation suggested by Wang et al. (2021) is that after a negative leader propagates for some time, it may transform to a positive leader under the so-called leader polarity reversal mechanism (Shi et al., 2018), and the later the polarity reversal occurs, the smaller the positive charges are left for the positive leader, and the weaker the resultant RS is.

It has long been reported that positive RSs are often preceded by extensive intracloud discharges (Fuquay, 1982; Kong et al., 2008; Saba et al., 2009). From the results of this study, we can infer that such positive RSs are unlikely very strong.

The same is true for subsequent RSs in positive CG flashes. Subsequent RSs in positive CG flashes rarely occur in the same channel as the first RS, but still they are usually much weaker than the first RS (Wu et al., 2020). One reason is that subsequent RSs in positive CG flashes are usually associated with positive leaders developing from

negative leader channels (Wu et al., 2020; Yuan et al., 2020), so they also tend to occur at a location far away from the lightning initiation location, similar to positive first RSs occurring a long time after the lightning initiation.

## 5. Conclusion

In this paper, we analyzed peak currents of first RSs in about 700 positive CG flashes observed by the FALMA in one winter season in the Hokuriku region of Japan. We focused on investigating relationships between peak currents of positive RSs and their waveform characteristics and other discharge processes. The major findings are summarized as follows.

Peak currents of positive RSs are positively correlated with E-change waveform parameters of RS pulses, including pulse width, rise time, fall time and half-peak width, with the rise time having the strongest correlation.

Positive RSs associated with positive and negative PB pulses are equally common, and peak currents of these two types of RSs have overall similar distributions. However, the strongest positive RSs are more likely to be associated with positive PB pulses (the same polarity as positive RSs). Peak currents of positive RSs do not have clear correlation with amplitudes of PB pulses.

Peak currents of positive RSs are closely related with the time difference between the lightning initiation and the first RS. Strong positive RSs are usually associated with small time differences, which is true for RSs associated with both polarities of PB pulses.

Peak currents of positive RSs are also related with amplitudes of preceding leader pulses. Out of 674 positive RSs, 232 are preceded by positive pulses, and only 15 are preceded by negative pulses. In the remaining 427 cases, there are no clear pulses or the pulses have mixed polarities. For positive RSs preceded by positive pulses, amplitudes of preceding pulses are positively correlated with peak currents of positive RSs. Comparison of preceding pulses on land and on the sea indicates that preceding pulses are more likely to be produced by upward negative connecting leaders.

Strong positive RSs with peak currents larger than 150 kA are analyzed and are compared with strong negative RSs. It has been reported that strong negative RSs produce abnormal E-change waveforms, making them difficult to be identified by lightning location systems, but waveforms of strong positive RSs do not have abnormal features. Compared with strong negative RSs, strong positive RSs are more common and are more likely to carry extremely large currents. Strong positive RSs tend to occur more frequently on the sea, just like normal winter lightning, while strong negative RSs are more likely to occur on land.

If we look at a few of the strongest positive RSs, we can see that they usually have very small time differences (smaller than 10 ms) with the lightning initiation. In other words, the strongest positive RSs usually occur in a very short period after the lightning initiation. The strongest positive RSs are also more likely to be associated with positive PB pulses. We can also infer that these strongest positive RSs are usually preceded by a fast downward positive leader with a speed on the order of $10^6$ m/s.

Based on the above results, we suggest that a strong downward electric field is essential for producing strong positive RSs. A large positive charge region is always necessary for such a downward electric field. For strong positive strokes starting with positive PB pulses, a small negative charge region may exist below the large positive charge region, and the initial positive leader starts from a location between the two charge regions, propagating directly downward to the ground. For strong positive strokes starting with negative PB pulses, the charge structure is more complicated; a small negative charge region surrounded by a large positive charge region is proposed, and the initial positive leader starts from the lower edge of the negative charge region, first propagating upward and then downward to the ground.

## Data Availability Statement

Data related with this paper can be found at https://doi.org/10.5281/zenodo.6629850.

**Acknowledgments**
This study was supported by the Ministry of Education, Culture, Sports, Science, and Technology of Japan (Grants 20H02129 and 21K03681).

## References

Brook, M., Nakano, M., Krehbiel, P., & Takeuti, T. (1982). The electrical structure of the Hokuriku winter thunderstorms. *Journal of Geophysical Research*, *87*(C2), 1207. https://doi.org/10.1029/jc087ic02p01207

Chen, L., Lu, W., Zhang, Y., & Wang, D. (2015). Optical progression characteristics of an interesting natural downward bipolar lightning flash. *Journal of Geophysical Research: Atmospheres*, *120*(2), 708–715. https://doi.org/10.1002/2014jd022463

Chronis, T., Koshak, W., & McCaul, E. (2016). Why do oceanic negative cloud-to-ground lightning exhibit larger peak current values? *Journal of Geophysical Research: Atmospheres*, *121*(8), 4049–4068. https://doi.org/10.1002/2015jd024129

Cummins, K. L., & Murphy, M. J. (2009). An overview of lightning locating systems: History, techniques, and data uses, with an in-depth look at the u.s. NLDN. *IEEE Transactions on Electromagnetic Compatibility*, *51*(3), 499–518. https://doi.org/10.1109/temc.2009.2023450

Fuquay, D. M. (1982). Positive cloud-to-ground lightning in summer thunderstorms. *Journal of Geophysical Research*, *87*(C9), 7131. https://doi.org/10.1029/jc087ic09p07131

Kong, X., Qie, X., & Zhao, Y. (2008). Characteristics of downward leader in a positive cloud-to-ground lightning flash observed by high-speed video camera and electric field changes. *Geophysical Research Letters*, *35*(5), L05816. https://doi.org/10.1029/2007gl032764

Li, S., Qiu, S., Shi, L., & Li, Y. (2020). Broadband VHF observations of two natural positive cloud-to-ground lightning flashes. *Geophysical Research Letters*, *47*(11), e2019GL086915. https://doi.org/10.1029/2019GL086915

Lyons, W. A., Uliasz, M., & Nelson, T. E. (1998). Large peak current cloud-to-ground lightning flashes during the summer months in the contiguous United States. *Monthly Weather Review*, *126*(8), 2217–2233. https://doi.org/10.1175/1520-0493(1998)126<2217:lpcctg>2.0.co;2

Marshall, T., Stolzenburg, M., Karunarathna, N., & Karunarathne, S. (2014). Electromagnetic activity before initial breakdown pulses of lightning. *Journal of Geophysical Research: Atmospheres*, *119*(22), 12558–12574. https://doi.org/10.1002/2014JD022155

Matsui, M., Michishita, K., & Yokoyama, S. (2019). Characteristics of negative flashes with multiple ground strike points located by the Japanese lightning detection network. *IEEE Transactions on Electromagnetic Compatibility*, *61*(3), 751–758. https://doi.org/10.1109/TEMC.2019.2913661

Nag, A., & Cummins, K. L. (2017). Negative first stroke leader characteristics in cloud-to-ground lightning over land and ocean. *Geophysical Research Letters*, *44*(4), 1973–1980. https://doi.org/10.1002/2016GL072270

Nag, A., & Cummins, K. L. (2018). Magnetic field risetimes of negative lightning first return strokes over land and ocean. *Geophysical Research Letters*, *45*(23), 13133–13141. https://doi.org/10.1029/2018GL080038

Nag, A., & Rakov, V. A. (2012). Positive lightning: An overview, new observations, and inferences. *Journal of Geophysical Research*, *117*(D8). https://doi.org/10.1029/2012jd017545

Nag, A., & Rakov, V. A. (2014). Parameters of electric field waveforms produced by positive lightning return strokes. *IEEE Transactions on Electromagnetic Compatibility*, *56*(4), 932–939. https://doi.org/10.1109/TEMC.2013.2293628

Orville, R. E., & Huffines, G. R. (2001). Cloud-to-ground lightning in the United States: NLDN results in the first decade, 1989–98. *Monthly Weather Review*, *129*(5), 1179–1193. https://doi.org/10.1175/1520-0493(2001)129<1179:ctglit>2.0.co;2

Orville, R. E., Huffines, G. R., Burrows, W. R., & Cummins, K. L. (2011). The North American lightning detection network (NALDN)—Analysis of flash data: 2001–09. *Monthly Weather Review*, *139*(5), 1305–1322. https://doi.org/10.1175/2010mwr3452.1

Peterson, M., & Lay, E. (2020). GLM observations of the brightest lightning in the americas. *Journal of Geophysical Research: Atmospheres*, *125*(23). https://doi.org/10.1029/2020jd033378

Pu, Y., Cummer, S. A., & Liu, N. (2021). VHF radio spectrum of a positive leader and implications for electric fields. *Geophysical Research Letters*, *48*(11), e2021GL093145. https://doi.org/10.1029/2021GL093145

Qie, X., Wang, Z., Wang, D., & Liu, M. (2013). Characteristics of positive cloud-to-ground lightning in da hinggan ling forest region at relatively high latitude, northeastern China. *Journal of Geophysical Research: Atmospheres*, *118*(24), 13393–13404. https://doi.org/10.1002/2013JD020093

Rison, W., Thomas, R. J., Krehbiel, P. R., Hamlin, T., & Harlin, J. (1999). A gps-based three-dimensional lightning mapping system: Initial observations in central new Mexico. *Geophysical Research Letters*, *26*(23), 3573–3576. https://doi.org/10.1029/1999GL010856

Rudlosky, S. D., & Fuelberg, H. E. (2010). Pre- and postupgrade distributions of NLDN reported cloud-to-ground lightning characteristics in the contiguous United States. *Monthly Weather Review*, *138*(9), 3623–3633. https://doi.org/10.1175/2010mwr3283.1

Saba, M. M. F., Campos, L. Z. S., Krider, E. P., & Pinto, O. (2009). High-speed video observations of positive ground flashes produced by intracloud lightning. *Geophysical Research Letters*, *36*(12), L12811. https://doi.org/10.1029/2009gl038791

Saba, M. M. F., Schulz, W., Warner, T. A., Campos, L. Z. S., Schumann, C., Krider, E. P., et al. (2010). High-speed video observations of positive lightning flashes to ground. *Journal of Geophysical Research*, *115*(D24). https://doi.org/10.1029/2010jd014330

Schumann, C., Saba, M. M. F., da Silva, R. B. G., & Schulz, W. (2013). Electric fields changes produced by positives cloud-to-ground lightning flashes. *Journal of Atmospheric and Solar-Terrestrial Physics*, *92*, 37–42. https://doi.org/10.1016/j.jastp.2012.09.008

Shi, D., Wang, D., Wu, T., & Takagi, N. (2019). Correlation between the first return stroke of negative cg lightning and its preceding discharge processes. *Journal of Geophysical Research: Atmospheres*, *124*(15), 8501–8510. https://doi.org/10.1029/2019JD030593

Shi, D., Wang, D., Wu, T., Thomas, R. J., Edens, H. E., Rison, W., et al. (2018). Leader polarity-reversal feature and charge structure of three upward bipolar lightning flashes. *Journal of Geophysical Research: Atmospheres*, *123*(17), 9430–9442. https://doi.org/10.1029/2018jd028637

Ushio, T., Kawasaki, Z.-I., Matsuura, K., & Wang, D. (1998). Electric fields of initial breakdown in positive ground flash. *Journal of Geophysical Research*, *103*(D12), 14135–14139. https://doi.org/10.1029/97jd01975

Velde, O. A., Montanyà, J., Soula, S., Pineda, N., & Mlynarczyk, J. (2014). Bidirectional leader development in sprite-producing positive cloud-to-ground flashes: Origins and characteristics of positive and negative leaders. *Journal of Geophysical Research: Atmospheres*, *119*(22). https://doi.org/10.1002/2013jd021291

Wacker, R. S., & Orville, R. E. (1999). Changes in measured lightning flash count and return stroke peak current after the 1994 u.s. national lightning detection network upgrade: 1. Observations. *Journal of Geophysical Research*, *104*(D2), 2151–2157. https://doi.org/10.1029/1998jd200060

Wang, D., & Takagi, N. (2011). A downward positive leader that radiated optical pulses like a negative stepped leader. *Journal of Geophysical Research*, *116*(D10), D10205. https://doi.org/10.1029/2010jd015391

Wang, D., Wu, T., & Takagi, N. (2018). Charge structure of winter thunderstorm in Japan: A review and an update. *IEEJ Transactions on Power and Energy*, *138*(5), 310–314. https://doi.org/10.1541/ieejpes.138.310

Wang, D., Zheng, D., Wu, T., & Takagi, N. (2021). Winter positive cloud-to-ground lightning flashes observed by lma in Japan. *IEEJ Transactions on Electrical and Electronic Engineering*, *16*(3), 402–411. https://doi.org/10.1002/tee.23310

Wu, T., Takayanagi, Y., Funaki, T., Yoshida, S., Ushio, T., Kawasaki, Z.-I., et al. (2013). Preliminary breakdown pulses of cloud-to-ground lightning in winter thunderstorms in Japan. *Journal of Atmospheric and Solar-Terrestrial Physics*, *102*, 91–98. https://doi.org/10.1016/j.jastp.2013.05.014

Wu, T., Wang, D., Huang, H., & Takagi, N. (2021). The strongest negative lightning strokes in winter thunderstorms in Japan. *Geophysical Research Letters*, *48*(21). https://doi.org/10.1029/2021gl095525

Wu, T., Wang, D., & Takagi, N. (2018a). Lightning mapping with an array of fast antennas. *Geophysical Research Letters*, *45*(8), 3698–3705. https://doi.org/10.1002/2018GL077628

Wu, T., Wang, D., & Takagi, N. (2018b). Locating preliminary breakdown pulses in positive cloud-to-ground lightning. *Journal of Geophysical Research: Atmospheres*. https://doi.org/10.1029/2018jd028716

Wu, T., Wang, D., & Takagi, N. (2020). Multiple-stroke positive cloud-to-ground lightning observed by the falma in winter thunderstorms in Japan. *Journal of Geophysical Research: Atmospheres*, *125*(20), e2020JD033039. https://doi.org/10.1029/2020JD033039

Wu, T., Wang, D., & Takagi, N. (2021). Compact lightning strokes in winter thunderstorms. *Journal of Geophysical Research: Atmospheres*, *126*(15), e2021JD034932. https://doi.org/10.1029/2021JD034932

Yuan, S., Qie, X., Jiang, R., Wang, D., Sun, Z., Srivastava, A., & Williams, E. (2020). Origin of an uncommon multiple-stroke positive cloud-to-ground lightning flash with different terminations. *Journal of Geophysical Research: Atmospheres*, *125*(15). https://doi.org/10.1029/2019jd032098

Zhang, Y., Zhang, Y., Lu, W., & Zheng, D. (2013). Analysis and comparison of initial breakdown pulses for positive cloud-to-ground flashes observed in Beijing and Guangzhou. *Atmospheric Research*, *129–130*, 34–41. https://doi.org/10.1016/j.atmosres.2013.03.006

Zheng, D., Wang, D., Zhang, Y., Wu, T., & Takagi, N. (2019). Charge regions indicated by LMA lightning flashes in Hokuriku's winter thunderstorms. *Journal of Geophysical Research: Atmospheres*, *124*, 7179–7206. https://doi.org/10.1029/2018jd030060

Zhu, Y., Rakov, V., & Tran, M. (2016). A study of preliminary breakdown and return stroke processes in high-intensity negative lightning discharges. *Atmosphere*, *7*(10), 130. https://doi.org/10.3390/atmos7100130

Zhu, Y., Rakov, V. A., Mallick, S., & Tran, M. D. (2015). Characterization of negative cloud-to-ground lightning in Florida. *Journal of Atmospheric and Solar-Terrestrial Physics*, *136*, 8–15. https://doi.org/10.1016/j.jastp.2015.08.006